Larhyss Journal, ISSN 1112-3680, n°60, Dec 2024, pp. 189-211

APPLICATION OF ELECTRICAL RESISTIVITY TOMOGRAPHY (ERT) FOR UNDERSTANDING BEDROCK ENVIRONMENTS AND IMAGING GROUNDWATER CONTAMINATION ZONE IN BURKINA FASO - WEST AFRICAN SAHEL

FAYE M.D.*, BIAOU A.C., MOUNIROU L.A., DOULKOM P.A.M., KOITA M., YACOUBA H.

Laboratory of Water, Hydro-Systems and Agriculture (LEHSA), International Institute for Water and Environmental Engineering (2iE) Rue de la Science – 01 PO BOX 594 Ouagadougou 01 - Burkina Faso

(*) moussa.faye@2ie-edu.org

Research Article – Available at http://larhyss.net/ojs/index.php/larhyss/index
Received January 3, 2024, Received in revised form November 22, 2024, Accepted November 24, 2024

ABSTRACT

In Burkina Faso, the quality of groundwater is increasingly threatened by both anthropogenic and natural factors, posing a significant challenge for the country. This degradation is particularly concerning in rural areas, where the abandonment of boreholes is observed, and a failure rate of 40% for drilling operations has been noted, compromising the water access rate of 80% set for 2015, which has still not been achieved. Agriculture, livestock farming, mining, and industry are the primary activities influencing water quality in the study area.

In the Sissili region, groundwater is often found in weathered layers and follows preferential pathways such as fractures. Therefore, the chemical composition of these waters is strongly related to the mineralogy of the parent rock and weathering processes, yet the structural complexity of aquifers remains poorly understood. The distance between a water point and the contamination source, as well as the depth of the superficial aquifer, are two crucial criteria for determining contamination.

This study aims to map the aquifers and identify contaminated areas. To achieve this, a geoelectrical method was applied using 10 electrical panels around polluted boreholes, over distances ranging from 360 to 720 meters depending on the locations. Through a finite difference algorithm and least squares inversion, this technique allows for visualizing resistivity variations, revealing contaminated zones in our case at depths of 10 to 20 meters, primarily in the second geological layer. It is sensitive to influencing properties such as electrical conductivity and helps identify pockets of contaminated groundwater.

In non-contaminated areas, the first layer appears to act as a filter. The results obtained provide a better understanding of basement aquifers, which is essential for more effective water resource management.

Keywords*:* Geophysics, Crystalline Basement, Electrical Resistivity Tomography, Groundwater Pollution

INTRODUCTION

The resolution of issues related to improving water access and addressing water contamination remains an ongoing discussion (Remini, 2010; Ayari and Ayari, 2017; Baba Hamed, 2021; Ihsan and Derosya, 2024). Rapid rural growth leads to a high demand for water, raising the question of how feasible it will be to ensure the availability of clean and uncontaminated water in an African city (Dos Santos, 2006; Ajeagah and Bissaya, 2017; Aroua 2022; 2023).

This phenomenon is particularly evident in basement areas, where the search and exploitation of groundwater in basement formations have remained at a preliminary stage (Courtois et al., 2010; Faye et al., 2020; Faye et al., 2022; Faye et al., 2023; Lachassagne et al., 2011; Nakolendousse et al., 2009; Sako et al., 2018; Sawadogo et al., 2023; Sawadogo et al., 2023; Soro et al., 2017; Soro et al., 2020). Groundwater is closely linked to the geology of the rocks they traverse or contain (De Lasme et al., 2015; Later and Labadi, 2024). Hence, it is essential to examine the main geological formations present to understand their influence on groundwater quality. (Belhadj et al., 2017; Faye et al., 2023).

Many countries have developed their own methods, adapted to local conditions, often drawing inspiration from existing methods. One can cite, for example: Noronha et al., (2000) in Portugal; Aboyeji et Eigbokhan, (2016) ; Ikem et al., (2002) ; Majolagbe et al., (2017) ; Oluseyi et al., (2014) ; Osibanjo et Majolagbe, (2012) in Nigéria ; Penant, (2016) in Bénin.

The state of knowledge regarding groundwater remains limited in West Africa, particularly in Burkina Faso. The extent of aquifer pollution is not clearly defined or well understood due to the discontinuity of the geological fracture network. To characterize it, Ahoussi et al. (2012), Ayouba Mahamane and Guel (2015a), Chemseddine et al. (2010), Dakoure (2003), Faye et al. (2020), Hounsinou et al. (2015), Ikem et al. (2002), Larissa Eba et al. (2016), Lasm (2000), Loukman et al. (2017), Mahamane and Guel (2015), Mahamat et al. (2015), Mfonka et al. (2015), Nkhuwa (2003), Rabilou et al. (2018), Soncy et al. (2015), Soro et al. (2011), Souley Moussa et al. (2019), Vadde et al. (2018), Wu et al. (2017), Zerhouni et al. (2015), and Zhang et al. (2019) use several different approaches. These approaches reveal that groundwater pollution is predominantly of anthropogenic origin. Unfortunately, most water points are not regularly monitored, and the population obtains water from facilities whose water quality is unknown. The average water resources amount to 850 m^3 per year per inhabitant, slightly below the threshold of water scarcity, which is 1000 m^3 per year per inhabitant (Valfrey-Visser and Rama, 2012).

It is observed that rock formations with high arsenic content contribute to this pollution (Abdou Babaye et al., 2017; Ayouba Mahamane and Guel, 2015b; Faye et al., 2020; Larissa Eba et al., 2016). If the importance of fracturing is no longer in question, the problem of locating faults and pollution remains unresolved. In the Sissili sub-basin, a selection of 206 boreholes was made. The results show a contamination rate of 30% in boreholes by toxic elements, heavy metals, metalloids, micropollutants, etc., leading to their abandonment by the population (Faye et al., 2020). Additionally, 40% of the boreholes are either negative or have non-productive flow rates (less than 1 m^3/h) (Faye et al., 2023; Savadogo, 1984). This situation is partly due to the lack of thorough studies conducted since 1984. This has led to contamination from discharge related to activities carried out around water points and the nonexistent sanitation system, which negatively impacts the lives of populations. This discharge accumulates on the ground, polluting surface waters, and through percolation, the contamination reaches the groundwater aquifer, altering its physicochemical characteristics. Access to this groundwater resource is achieved through wells or boreholes that tap into waters present in weathered materials and fissured aquifers beneath them. However, the complexity lies in the heterogeneity of the geometric structure, which remains poorly understood, especially regarding contamination knowledge.

For a less costly solution, 2D electrical resistivity tomography using geoelectrical techniques is employed to characterize the aquifer and evaluate contamination (Cuong et al., 2016; Cuong et al., 2019; Dahlin, 2004; De Clercq, 2021; Metwaly et al., 2014; Nakolendousse et al., 2009; Soro et al., 2017). It allows for more precise determination of the positions of geological discontinuities and the localization of areas with high hydrogeological interest. It also takes into account the contrast in electrical conductivity, which varies based on the type of geological formation, water content, temperature, and quality (Metwaly et al., 2014; Parasnis, 2012, 1997). Indeed, water quality and content control electrical conductivity, so an increase in ions due to contamination is automatically detected according to the empirical relationship of (Waxman and Smits, 1968). Therefore, we will see if this 2D method is better suited to the geological context. According to Vouillamoz et al., (2015) using a coupled hydrogeology/geophysics approach can compensate for the lack of data and significantly reduce uncertainties related to aquifer knowledge. This approach will contribute to a better understanding of basement aquifers for improved decision-making. This approach will contribute to a better understanding of basement aquifers, leading to more informed decision-making.

Study Area

The Sissili sub-basin, covering an area of 7,559 km^2, has a triangular shape, as illustrated in (Fig.1a). It extends between longitudes 1° and 2° West and latitudes 11° and 12° North. It is traversed by the Sissili River, which originates in the locality of Thyou in the north of the basin. The basin entirely or partially covers 12 municipalities and 3 provinces (Faye et al., 2020; Faye et al., 2023).

The total resident population is estimated at 1,695,863 inhabitants. The active population represents approximately 50.98%. The population density is estimated at 79 inhabitants per km^2, implying a high demand for natural resources by the population (INSD, 2020).

According to the (Conseil national de prospective et de planification stratégique, 2005), urbanization is rapidly increasing and carries many uncertainties.

Regarding land use, agricultural areas are the most significant in terms of spatial occupation. Pastoral or natural zones cover vast expanses of natural formations, serving as grazing areas for small ruminants during the winter season. Lastly, there are wetland areas (Faye et al., 2020).

Significant land use changes were observed from 1982 to 2011, with shrub savanna being the dominant unit, covering 40.65% of the total area. According to Yameogo et al., (2020), Landsat images show a land use matrix from 2012 to 2018, in which fields represented more than half of the watershed in 2018, accounting for 57.84% (Fig. 2). Between 2002 and 2018, notable transformations included the conversion of 1.800 ha of riparian formation, 43.498 ha of tree savanna, and 66.557 ha of shrub savanna into fields. Additionally, a decrease was observed in 78.30 ha of fields, 1.826 ha of tree savanna, and 830.56 ha of shrub savanna in favor of riparian formation. Similarly, 6.811 ha of fields, 18.379 ha of shrub savanna, and 1.757 ha of riparian formation were converted into tree savanna. Shrub savanna increased at the expense of 4.812 ha of fields, 2.461 ha of riparian formation, and 27.788 ha of tree savanna. Between 2002 and 2018, the areas of land use units that expanded include fields, habitats, water bodies, and bare or eroded areas, representing 31.64%, 0.09%, 0.07%, and 0.02% of the total watershed area, respectively. In contrast, vegetative formations such as shrub savanna (-16.11%), tree savanna (-14.58%), and riparian formation (-1.13%) experienced a decrease in their area.

The soil acts as a reservoir of water and nutrients for plants, influencing runoff, infiltration, and the storage of rainwater. In the sub-basin, there are various types of soils with distinct characteristics. First, there are deep, poorly evolved soils (>120 cm), with deficient internal drainage, composed of alluvium. Next, there are the group of raw mineral soils (<10 cm), with no water retention capacity. Finally, there are the hydromorphic soils, which have good water retention capacity (Hien et al., 1996; Savadogo, 1975).

Rainfall has been trending downward over the past two decades (Paturel et al., 2010). This fact has been supported by a study conducted by the Meteorological Department, which investigated climate variability over normal years using 49 meteorological stations. The study highlighted a general southward migration of the 600 mm and 900 mm isohyets. Consequently, daily rainfall is estimated at 151 mm for a return period of 10,000 years. There are two Sudanian climatic periods observed: a dry season from November to April and a rainy season from May to October.

The study area benefits from abundant hydrography due to its relief and high rainfall in the region. The area is traversed by the Sissili River (a tributary of the Nazinon), which gives its name to the province. It has a drainage density of 0.74 km^{-1} and a concentration time of 73.53 hours. The river is 322 km long, with the first 42 kilometers having an average slope of 1.48 m/km. This slope then gentles over the next 125 km to the Nebou station, where it becomes 0.663 m/km before flowing into Ghana (Dahl et al., 2018; Faye et al., 2023; Giovenazzo et al., 2018; Savadogo, 1984).

The severe drought of the 1970s had significant consequences on the vegetation cover in the area. It led to soil erosion, and water bodies were affected by siltation. Currently, the vegetation cover consists of shrub savanna, with the presence of agroforestry parks and gallery forests along the watercourses.

The relief of the Sissili region is characterized by small rocky massifs, small hills resembling elephant backs, mainly composed of granite, and barely noticeable ridges. The hypsometric curve provides a perspective view of the sub-basin's topography, revealing a relatively steep slope with moderately sloped areas in places. This topography promotes erosion, particularly in the upper part of the basin. Minimum altitudes represent the levels of valleys and lowlands, while maximum altitudes correspond to peaks including higher elevations. The Sissili sub-basin has an average altitude of 321.43 meters and an average slope of 2.03 m/km, resulting in an overall slope index of 0.42 m/km.

From a geological perspective, the Sissili sub-basin exhibits three types of geological formations that are productive in terms of water resources (Fig. 1b). Firstly, there are migmatites, which consist of an intimate mixture of weathered materials and nebulae without stratifications. Secondly, there is a mixture of gneiss or mica schists with granites that can be distinguished with the naked eye. Lastly, there are gneisses with feldspathic facies. Secondly, granite formations are observed, varying greatly in terms of their degree of fracturing and the size of their minerals. Thirdly, there are basic rocks and quartz veins present, including amphiboles, granodiorites, and dolerites. Additionally, there are rock formations with high arsenic content (Dahl et al., 2018; Faye et al., 2022; Faye et al., 2023; Giovenazzo et al., 2018; Savadogo, 1975b; Savadogo, 1975).

The study of fracturing reveals predominant directions, mainly NE-SW > NW-SE, where open joints are observed, as well as directions of E-W > N-S, where closed joints are found.

From a hydrogeological perspective, the hydraulic productivity of basement aquifers varies depending on the encountered aquifer formations. Formations such as granodiorites, tonalites, and quartziferous diorites are characterized by higher hydraulic productivity, with flow rates exceeding 20 m^3/h. Next are formations like orthogneisses, mica schists with kyanite, garnet-bearing leptynites, garnet-bearing mica schists, sillimanites, and staurolites, which exhibit moderate productivity typically below 20 m^3/h. In contrast, volcano-sedimentary formations generally have lower hydraulic productivity. While it can exceed 5 m^3/h initially, this value may decrease due to progressive aquifer clogging. The least productive formations are usually found in intrusive plutons, where flow rates can be around 2 m^3/h or lower.

The hydrogeological profile exhibits a vertical structure composed, from top to bottom, of superficial layers ranging from 2m to 3m thick. The saprolite layer includes two sub-layers: the allotriite and the isaltrite, situated between 17 and 22 meters depth. The fractured bedrock is found at a depth of 18 to 20 meters. Finally, the intact bedrock is located at the base of the weathering profile, at a depth of 6 to 10 meters. This profile reflects the complexity of basement aquifers, with different layers possessing varying hydraulic properties.

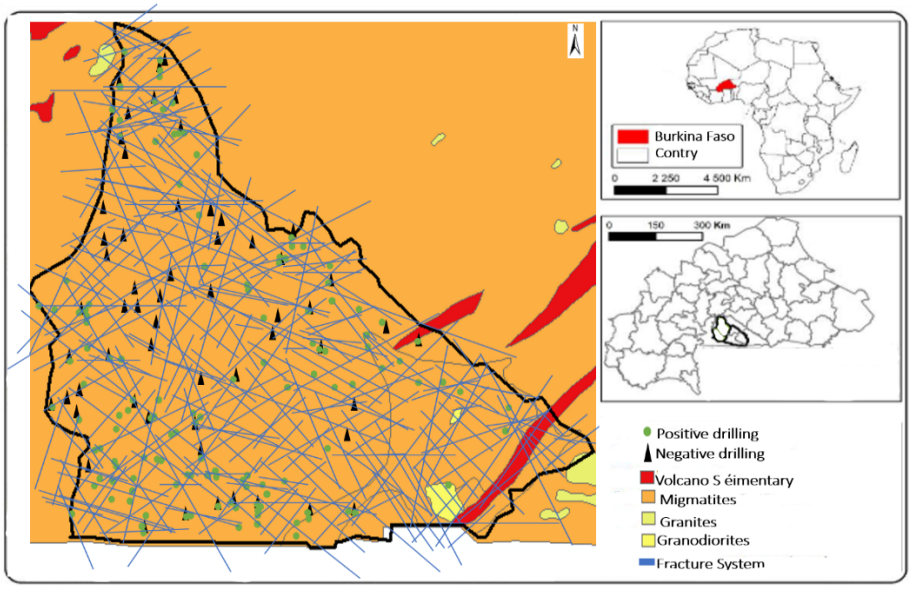

Figure 1a : Geographical location of the Sissili catchment area and Simplified geological map, distribution of fractures and water extraction points for positive boreholes (Faye et al., 2023).

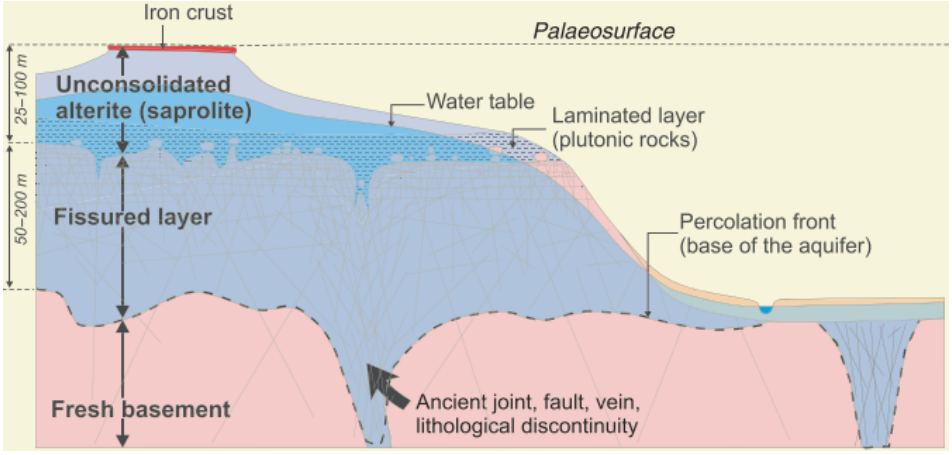

Figure 1b: New concept: Resource established in weathering profiles

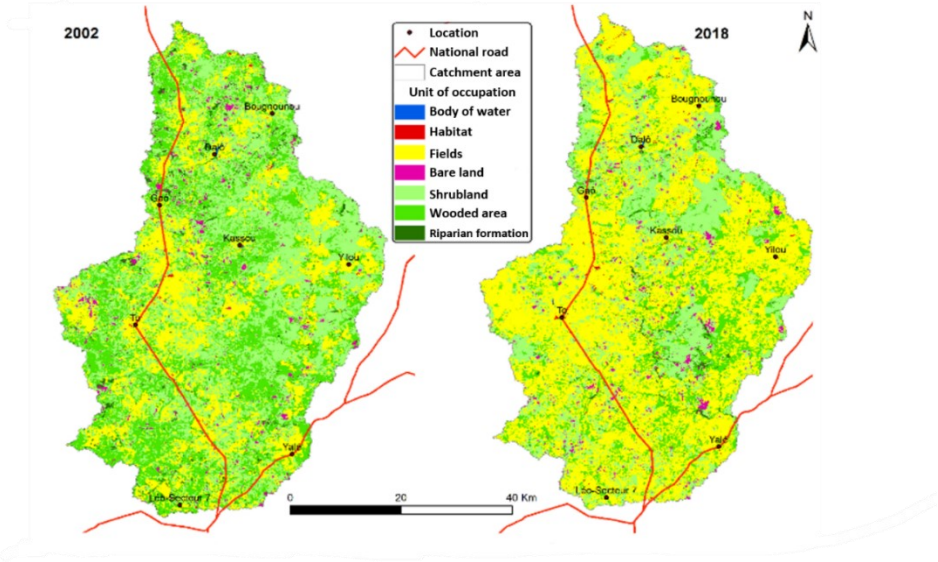

Figure 2: Land use dynamics between 2002 and 2018 (Yameogo et al., 2020)

MATERIAL AND METHODS

Groundwater Data Sampling and Analytical Method

To assess contamination in rural areas, a field campaign was launched to detect high levels of harmful chemicals in water across the 13 regions of Burkina Faso. Sampling was conducted in 58 boreholes equipped with hand pumps to ensure comprehensive coverage of the 13 municipalities, in accordance with standard norm recommendations.

For our study, 16 parameters were analyzed. Physical parameters were measured using a multiparameter device, HANNA HI 9828. Ions such as nitrate (NO_3^-), sulfate (SO_4^{2-}), nitrite (NO_2^-), orthophosphate (PO_4^{3-}), iron (Fe^{2+}), ammonium (NH_4^+), and fluoride (F^-) were quantified using molecular absorption spectrophotometry (Hach DR 3800). Sodium (Na^+) and potassium (K^+) ions were analyzed using flame atomic emission photometry. The method used to evaluate total cyanide involved spectrophotometry after hot mineralization. Trace elements and metals such as arsenic (As), lead (Pb), and zinc (Zn) were detected using microwave plasma atomic emission spectrometry (MP-AES 4210 Agilent). Quantification of carbonate ions, bicarbonate (HCO_3^-), and chloride (Cl^-) was performed using volumetric methods with sulfuric acid and silver nitrate, respectively.

Application of the Electrical Resistivity Method

The resistivity method has long been used to sample the linear part of the subsurface, such as current flow zones, while providing a measurement relative to the quantity (Metwaly et al., 2014, Lachache et al., 2023).

In our study, we employed the Wenner alpha and Wenner beta configurations. Indeed, (Alle, 2019; Roques, 2013) suggest the dipole-dipole configuration for basement zones. (Koussoube et al., 2000) previously used seismic refraction methods extensively, but these proved ineffective in the area due to the higher propagation velocity in the weathered layer compared to the underlying bedrock. For our case, we opted for synthetic modeling, also known as direct modeling, which is a numerical test used to select the appropriate survey configuration and inversion parameters. The choice of the optimal configuration depends on the structure to be imaged, background noise, and the sensitivity of the measuring device as defined by (Soro, 2017; Sognon et al., 2018). This modeling approach guided our selection of the electrical method and the chosen survey configuration.

In the field, resistivity measurements were conducted using a Syscal IRIS Instruments system with 72 electrodes and its associated accessories. The electrodes were spaced 5 meters apart, operating in a multi-electrode configuration with a maximum of four spreads (18 electrodes per spread). Depending on the assigned sequence, the system injected current and measured the resulting potential difference through cables in contact with the ground via stainless steel stakes.

The tomography was conducted using a Roll Along method, where the device was moved halfway after the 72nd electrode. This measurement approach provides a balanced compromise between investigation depth and field implementation. Selecting the appropriate device is crucial for achieving better resolution of discontinuities. The 2D imaging measures apparent resistivity, which is inverted to establish a model of the subsurface structure and electrical properties (Boucher et al., 2006; Boucher, 2007; Loke, 2004; Metwaly et al., 2014).

The data acquisition sequences were inverted and interpreted using the Res2DInv software. This process involved using the measured apparent resistivity values to determine soil models, aiming to minimize the difference between the calculated pseudo-section for a given soil model and the measured pseudo-section in the field. The quality of inversion, which minimizes this difference, is assessed using the Root Mean Squared (RMS) error, an estimator of uncertainty. RMS measures the discrepancy between the calculated apparent electrical resistivities and the measured resistivities using the least squares criterion (Hacini, 2006). To achieve a model that mathematically reproduces the measured apparent resistivities, it is essential for the RMS to be as low as possible, typically evaluated within a 10% range (Soro, 2017).

The inversion develops a model of the subsurface structure and stratigraphy in terms of electrical properties. The inversion process begins with data preprocessing, involving the acquisition of device data programmed using Prosys II software and output in *.DAT

format. This process reveals that the number of lines correlates directly with the number of eliminated values, resulting in potentially different line counts across files. Subsequently, outliers are removed, and defective electrodes may be excluded. For Roll Along surveys, consideration must be given to the coordinates of the first electrode. Processing was facilitated using X2IPI software.

A range of resistivity values was selected using color codes to differentiate resistivity and facilitate the interpretation of the inversion results. This approach was informed by the analysis of electrical resistivity logs proposed by (Soro, 2017). It enabled the assignment of specific ranges of electrical resistivities to each layer of the alteration profile. These logs reveal that within a given alteration profile, resistivity values vary with depth within the same layer, indicating its heterogeneity. This resistivity is affected by porosity, water volume, ion concentration, and subsurface composition. These results will be used to delineate and map features such as contamination with electrically conductive characteristics. Thus, resistivity values in the saprolite layer range from 56 Ω·m to 228 Ω·m, in the fractured layer from 228 Ω·m to 871 Ω·m, and in the unaltered bedrock layer from 871 Ω·m to 3727 Ω·m.

The subsurface resistivity affects the porosity and ionic content of water; therefore, resistivity data can be used to delineate electrically conductive contamination zones.

In total, 4 electrical panels from the Roll Along surveys (totaling 10 panels) were conducted. Measurements were taken at four sites (see Fig. 3). The investigations covered distances of 720 m at Kada, Thyou, and Sissili Mossi, and 360 m at Tiakané. These measurements were taken near existing boreholes and perpendicular to fractures.

The significance of positioning the measurement section near these boreholes lies in using the lithological data from these boreholes as references to assess the geological reality of the alteration profile models derived from the inversion of apparent resistivities. This approach aids in validating the geological models obtained and aims to establish connections between the responses of geoelectric techniques and various lithological parameters.

Following this approach, we defined the alteration thicknesses of borehole lithologies based on the data acquired at our level. Subsequently, resistivity values from the tomography data inversion were assigned to these thicknesses. This process allows us to classify them geologically based on the correspondence of resistivity ranges according to the layers of the alteration profile established by the results of electrical logging investigations.

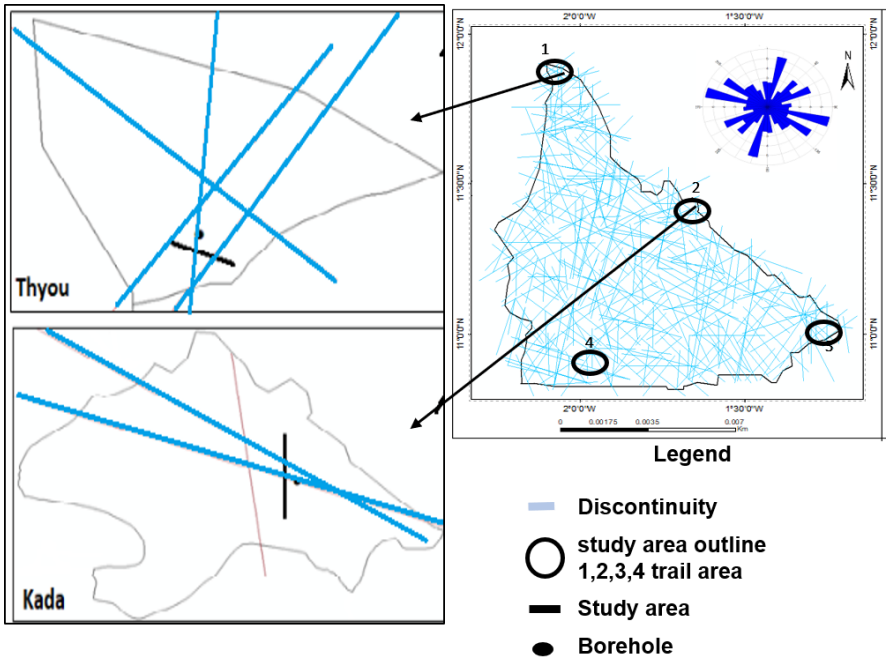

Figure 3: Presentation of the ERT zones in the commune of Kada and Thyou

RESULTS

The inversion results of the ERT applied to the four sites generally follow a north-south direction, intersecting with existing boreholes (Fig. 4). The sections represent resistivities in color: low resistivities are shown in blue (9.21 Ω.m to 228 Ω.m); high resistivities in green (228 Ω.m to 871 Ω.m), representing the fractured zone; and very high resistivities in red-orange (871 Ω.m to 1000 Ω.m), indicating the intact bedrock. The resistivity threshold selected by the model is 228 Ω.m for distinguishing between the altered and fractured zones, and 871 Ω.m for the boundary between the fractured zone and the intact rock.

The Kada section, after reclassifying the resistivities, revealed a profile with three continuous layers corresponding to different geological layers of the subsurface: saprolite, the fractured zone, and intact rock, with resistivity ranges varying from 16.2 Ω.m to 36,258 Ω.m. Subsequently, the lithological profile was superimposed on the section. It was observed that the geophysical boundary is approximately 15 meters below that indicated by borehole lithologs. Additionally, the resistivity section shows three resistant bodies within the saprolite. Two of these bodies are exposed at the surface, while the third is located along the central axis at about 12 meters depth. The two surface-resistant bodies are lateritic crusts. They are followed by a conductive compartment characterized by an alteration layer with a clayey tendency. In the center of the section, a

layer can be noted between depths of 10 and 18 meters on the borehole lithologs, corresponding to depths from 320 to 312 meters over a length of 80 meters.

The Koukin section represents continuous layers corresponding to different geological subsurface layers with resistivity ranges varying from 7.42 Ω.m to 72,000 Ω.m. Within the layers identified by the imaging, there is a surface layer at only one location with resistivities ranging from 301 Ω.m to 400 Ω.m. The thickness of this layer is 9 meters, corresponding to a depth of 345 meters. It is characterized by resistivity ranging from 7.42 Ω.m to 228 Ω.m, extending to a depth of 27 meters, corresponding to a depth of 333 meters on the section. The layer is characterized by a horizon of conductive arenas with variations in the surrounding clay layer, averaging 100 Ω.m. The thickness of the observed alteration layer is generally greater than 40 meters across the entire section. However, we note an inconsistency with the borehole lithologs, which show five continuous layers during drilling, while the section shows three layers.

The Tiakané section represents resistivity ranges varying from 9.60 Ω.m to 93,000 Ω.m. Furthermore, the resistivity section shows a resistant body (resistivity greater than 871 Ω.m) in the saprolite. This resistant body, which surfaces, is part of the lateritic cuirass at approximately 25 meters depth over a distance of 20 meters, as observed on the field. The three formations described by the classic conceptual model in basement zones are present. The Sissili Mossi section illustrates resistivity ranges varying from 11.68 Ω.m to 72,000 Ω.m with an RMS of 4.2%. Analysis of the section shows a resistant body (resistivities greater than 871 Ω.m in places) that extends across almost the entire surface. This resistant body has a thickness varying between 4 and 10 meters. Below it, a conductive compartment with resistivity oscillating between 21.2 and 228 Ω.m and a thickness of about 20 meters is observed. Additionally, the section imagery reveals that the fresh rock is intersected by a conductive corridor (approximately 20 meters wide).

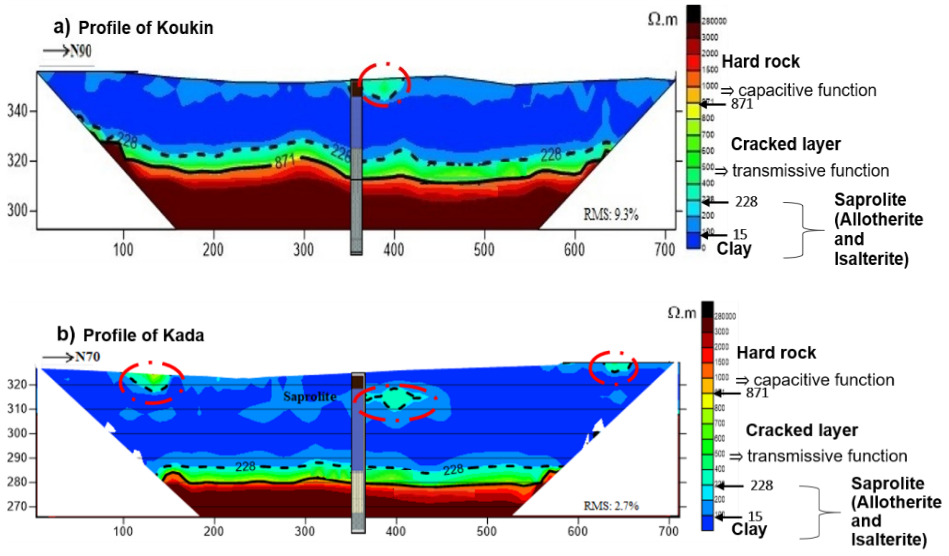

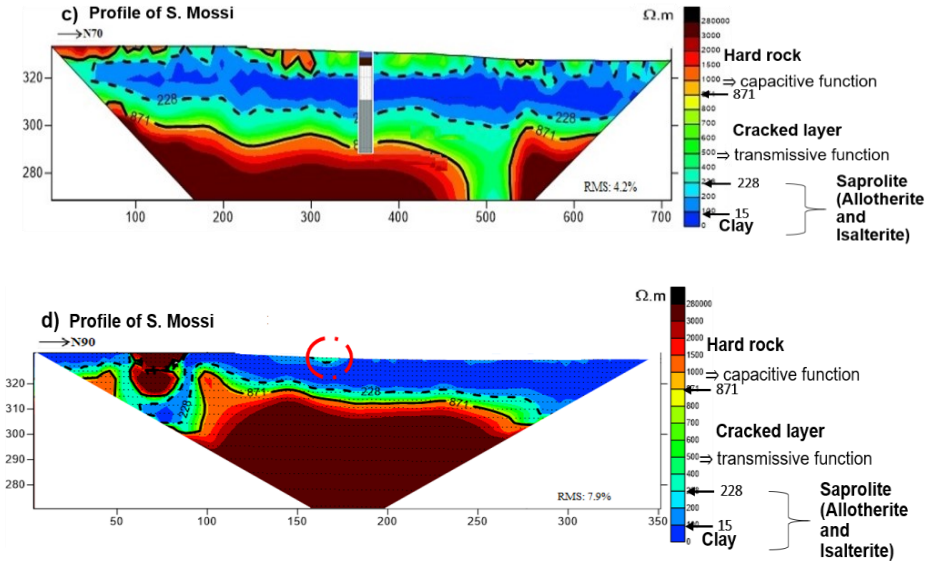

Figure 4: Panel of Electrical Resistivity Tomography (ERT) Profiles

DISCUSSION

The results of the inversion of tomography data are represented by Fig. 4, with corresponding RMS error values of 2.7%, 9.3%, 7.9%, and 4.2%. These low RMS values are explained by the fact that outlier data are eliminated during preprocessing, so the filtering results in a smoothed data section. If we had values above 20%, it would suggest the presence of small air pockets resulting from the explosion of certain minerals within the bedrock aquifer. According to (Lghoul et al., 2012) the acceptable RMS tolerance value should be less than 20%, considering prior knowledge to choose the most realistic model to retain.

The difference in the geophysical boundary of 15 m below that indicated by lithologs observed in the Kada section (Fig. 4b), 3 m below the Koukin section (Fig. 4a), and 10 m below the Sissili Mossi section (Fig. 4c) is explained by hydrogeologists as either due to the lack of precise lithologs for the boreholes. (Cuong et al., 2016) in Vietnam describe it as being water-saturated clay materials present at the surface and extending up to 10 m, also noting that the upper layer can be composed of bearing rock. In Fig. 4, this coincides with the blue-colored part and resistivity range of 9.21 Ω.m to 228 Ω.m. Additionally, in the inversion results, the change in resistivity from one layer to another does not necessarily correspond to a change in terrains but rather to variations in water content within the same layer. However, by summing the thicknesses of the terrain layers in question on the lithologs, we obtain the thickness identified in the section.

There is indeed uncertainty regarding the actual depth of the base, either due to the difficulty in selecting an electrical resistivity threshold to delineate the base of the fractured layer. This can be explained by percolation theory, where decreasing fissure density at the base halts percolation. Consequently, it becomes challenging to distinguish the electrical resistivities of the base of the fractured layer from those of the intact rock (Soro, 2017).

The presence of rock in the center of the device in the Kada section (Fig. 4b), characterized by resistivity ranging from 228 Ω.m to 400 Ω.m, may indicate the presence of volcanic sedimentary rock. The layer at a single location with resistivities ranging from 301 Ω.m to 400 Ω.m in Koukin (Fig. 4a) and Sissili Mossi (Fig. 4c) is described as a probable area of anthropogenic contamination input. According to (Lghoul et al., 2012), this high resistivity separating the conductive layer at a given depth serves as an indicator of pollution due to its central position in the model, representing an anthropogenic pollutant. In this regard, the 2D profiles reveal the presence of pollutants with resistivity ranges varying between 1 Ω.m to 5 Ω.m in the superficial zone, between 20 Ω.m to 90 Ω.m in the altered zone, and greater than 90 Ω.m in the fresh rock as indicated in the red part of Fig. 4. From this, we can infer that apart from the fracture where the borehole is located, we have identified a corridor characterized by a layer more resistant than the alterites with resistivity ranging from 228 Ω.m to 871 Ω.m. Other fractures may be visible in a resistivity profile and could be more productive and visible on satellite images. (Faillat and Drogue, 1993) describe it as the presence of weathered granites, confirmed by the borehole log. Research conducted by(Faye et al., 2020) documented the state of pollution in the study area. Based on sampling results, these areas have shown levels of pollution exceeding Burkina's limits for micropollutants and heavy metals. This is corroborated by natural arsenic presence in Burkina Faso's subsurface as studied by (Bretzler et al., 2017). Furthermore (Faye et al., 2024) demonstrated the expected persistence of this pollution over the next 50 years if no action is taken. The 2D model has just imaged the described pollution. Activities around water points reveal that groundwater pollution is predominantly anthropogenic. Indeed, the presence of lateritic duricrust promotes runoff towards groundwater recirculation zones, becoming preferential recharge areas. Runoff water infiltrates here, leading to localized aquifer recharge. Unfortunately, most water points are not periodically monitored, and the population uses water sources with poor water quality. It would be valuable in future studies to repeat these tests at different times to observe any changes in resistivities.

In the Sissili section (Fig. 4c), the anomaly traversing the bedrock may indicate the presence of a tectonic fault. The depth of investigation does not definitively reveal the thickness or depth of this layer. Some authors like (Alle, 2019) assert that beyond 50 meters using the Wenner method, the base of the bedrock is not well identified when the altered zone is clayey, whereas dipole-dipole is more appropriate for deeper structures. We also observe discontinuity in this area in satellite images. The results obtained from this study provide a good compromise in terms of locating tectonic fractures on the Sissili field between remote sensing and ERT, though insufficient to draw definitive conclusions. This finding can be compared with other studies. (Soro, 2017) in Sanon using the same setup found no traces of tectonic fractures in their sections, whereas our

imagery shows an opening in the bedrock. (Akokponhoué et al., 2019) in Benin, in a similar bedrock environment, obtained results comparable to this section. However, they affirm that the 2D method can validate fractures but suggest it requires more experimentation in bedrock areas, considering the depth of investigation of the deployed device.

In general, the observation of inversion results indicates three easily identifiable layers in the bedrock zone: the saprolite, which can be divided into two sub-layers, the allochthonous sub-layer and the iso-alterite sub-layer, the fractured layer, and the intact bedrock, following the defined resistivity ranges mentioned earlier.

The tomography shows that laterites, cover thicknesses, etc., vary across different zones. Alteration thicknesses in lithologs range from 17 to 20 meters, while the geophysical model gives thicknesses ranging from 17 to 40 meters. However, (Courtois et al., 2010) estimates them between 20 meters and 31 meters in Burkina, whereas (Soro, 2017) estimates them between 13 meters and 21 meters in Sanon. Some authors attribute this difference to poor representation of lithologs during drilling, leading to uncertainty, or non-representative values assigned to different resistivities in the fractured zone. In other words, the armored ridges do not coincide with groundwater divides. Looking at the various figures, we can conclude that if the alteration thickness is significant, surface fractures cannot be identified by 2D methods. These results align with recent profiles described by (Courtois et al., 2010; Dewandel, 2019; Koita et al., 2010; Savadogo, 1984; Soro, 2017), which support that hydraulic parameters are related to the weathering process. This is justified by the fact that most boreholes are drilled at about a hundred meters depth, allowing them to capture secondary fractures. While the conceptual model described by (Lachassagne and Wyns, 2005) asserts that lineaments are represented by tectonic fractures, (Soro, 2017) argues that tectonic fracturing cannot be invoked as a genetic concept to explain the origin of secondary fissures in basement rocks.

But the question of whether to continue this method remains. The 2D tomography profile confirms those of the 1D profiles and goes beyond their limits, perfectly characterizing geological structures to define their geometry. However, ERT has limitations; for example, it struggles to identify fractures in altered and tectonic zones. According to the Wenner array, accurately identifying the depth limit of sound rock is challenging, as shown by the profiles of Sissili Mossi, Koukin, and Kada.

CONCLUSION

The study was conducted in an area where little research has been done previously, yet socio-economic activities are crucial. Unfortunately, these activities, combined with population growth and overexploitation of water resources, have led to groundwater pollution. The analysis revealed that anthropogenic impact plays a significant role in the degradation of groundwater quality, which is reflected in the nature and spatial distribution of polluted zones. The infiltration of pollutants over time leads to their accumulation, and as percolation continues, the receiving geological environment spreads this pollution. These observations are crucial for the planning of future boreholes.

The study also showed that differences in the composition and thickness of geological layers are likely responsible for many failures during drilling. In this context, the introduction of the 2D method has proven to be a powerful tool for groundwater prospecting. The techniques applied have allowed for the delineation of contaminated zones, with low resistivity values indicating affected areas in the saprolite, as corroborated by lithologies from boreholes and post-inversion data. In areas where pollution is not detected, it is likely that the upper layer acts as a natural filter. Additionally, the study highlighted a weathering profile consistent with recent models suggesting that hydraulic conductivity in basement environments is more due to weathering than to tectonic fractures. This methodology also presents some limitations, including limited spatial resolution, the influence of variations in soil conductivity, detection depth, difficulty in distinguishing between types of contamination, as well as the influence of terrain geometry, among others. For future studies, it is recommended to apply high-density techniques to enable more precise mapping of contamination pathways.

Declaration of competing interest

The authors declare that they have no known competing financial interests or personal relationships that could have appeared to influence the work reported in this paper.

REFERENCES

ABDOU BABAYE M.S., SANDAO I., SALEY M.B., WAGANI I., OUSMANE B. (2017). Hydrogeochemical Behavior and Contamination of Fractured Aquifer Waters of the Precambrian Basement in a Semi-Arid Environment (Southwest Niger), International Journal of Biological and Chemical Sciences, Vol. 10, No 6, pp. 2728-2743 (In French).

ABOYEJI O.S., AND EIGBOKHAN S.F. (2016). Evaluations of Groundwater Contamination by Leachates around Olusosun Open Dumpsite in Lagos Metropolis, Southwest Nigeria, Journal of Environmental Management, Elsevier, Vol. 183, pp. 333–341.

AHOUSSI K., OGA Y., KOFFI Y., KOUASSI A., SORO N., BIEMI J. (2012). Hydrogeochemical and Microbiological Characterization of Water Resources at a Technical Landfill Site (CET) in Côte d'Ivoire: Case of Kossihouen CET in the Abidjan District (Côte d'Ivoire), International Journal of Biological and Chemical Sciences, Vol. 5, No 6 (In French).

AJEAGAH G., BISSAYA R. (2017). Availability of water resources in Cameroon: ecoenvironmental potentialities and sustainable management by the population, Larhyss Journal, No 32, pp. 7-22. (In French)

AKOKPONHOUÉ N., YALO N., AKOKPONHOUÉ B., YOUAN TA M., AGBAHOUNGBA G. (2019). Contribution of Remote Sensing and Geophysics to Mapping Hydraulically Active Fractures in Basement Areas in Central-Western Benin: (Contribution of Remote Sensing and Geophysics to Mapping Hydraulically Active Fractures in the Central-Western Region of Benin), European Scientific Journal, Vol. 15, No 27 (In French).

ALLE I.C. (2019). Evaluation of Geophysical Implantation of Boreholes in Basement Areas in Tropical Environments (Benin, West Africa): Contribution of Electrical Resistivity Tomography for Hydrogeological Target Characterization, Doctoral Thesis, University of Abomey-Calavi, Cotonou, Benin (In French).

AROUA N. (2022). Long term city development versus water strategy in Al-Maghreb, Larhyss Journal, No 50, pp. 173-197.

AROUA N. (2023). Setting out urban water issues examples from Algeria and worldwide, Larhyss Journal, No 56, pp. 309-327.

AYARI K., AYARI A. (2017). For better governance of drinking water in Tunisian rural areas, Larhyss Journal, No 29, pp. 7-21. (In French)

BABA HAMED S. (2021). Impact of water pollution on public health and the environment in Oran, Larhyss Journal, No 45, pp. 203-222.

BELHADJ M.Z., BOUDOUKHA A., AMROUNE A., GAAGAI A., ZIANI D. (2017). Statistical characterization of groundwater quality of the northern area of the basin of Hodna, M'sila, southeastern Algeria, Larhyss Journal, No 31, pp. 177-194. (In French)

BOUCHER M. (2007). Estimation of the Hydrodynamic Properties of Aquifers by Proton Magnetic Resonance in Different Geological Contexts, from Sample to Hydrogeological Scale, Dissertation, University of Orléans, France (In French).

BOUCHER M., GIRARD J.-F., LEGCHENKO A., BALTASSAT J.-M., DÖRFLIGER N., CHALIKAKIS K. (2006). Using 2D Inversion of Magnetic Resonance Soundings to Locate a Water-Filled Karst Conduit, Journal of Hydrology, Elsevier, Vol. 330, No 3–4, pp. 413–421.

BRETZLER A., LALANNE F., NIKIEMA J., PODGORSKI J., PFENNINGER N., BERG M., SCHIRMER, M. (2017). Groundwater Arsenic Contamination in Burkina Faso, West Africa: Predicting and Verifying Regions at Risk, Science of the Total Environment, Elsevier, Vol. 584, pp. 958–970.

CHEMSEDDINE F., ABDERRAHMANE B., ABDELKADER R., ELIAS S. (2010). Hydrogeochemical Characterization of Groundwater in the Morsott-Laouinet Aquifer Complex (Northern Tébessa Region, Southeastern Algeria), Afrique Science, Revue Internationale des Sciences et Technologie, Vol. 5, No 2 (In French).

DE LASME O.Z., YOUAN TA M., BAKA D., ADOPO K.L., LASM T., OGA M.S. (2015). Quantitative evaluation and hydrogeochemical properties of groundwaters from precambrian rocks of san pedro area (southwestern Côte d'Ivoire), Larhyss Journal, No 23, pp. 183-201.

FASO B. (2025). National Council for Foresight and Strategic Planning (2005), National Prospective Study Burkina 2025 (In French).

COURTOIS N., LACHASSAGNE P., WYNS R., BLANCHIN R., BOUGAÏRE F.D., SOME S., TAPSOBA A. (2010). Large-Scale Mapping of Hard-Rock Aquifer Properties Applied to Burkina Faso, Groundwater, Vol. 48, No 2, pp. 269–283.

CUONG L.P., VAN THO L., JUZSAKOVA T. (2019). Aquatic Geochemistry Status in the South, Central, and Highland Regions of Vietnam, Environmental Science and Pollution Research, Springer, Vol. 26, pp. 21925–21947.

CUONG L.P., VAN THO L., JUZSAKOVA T., RÉDEY Á., HAI H. (2016). Imaging the Movement of Toxic Pollutants with 2D Electrical Resistivity Tomography (ERT) in the Geological Environment of the Hoa Khanh Industrial Park, Da Nang, Vietnam, Environmental Earth Sciences, Springer, Vol. 75, pp. 1–14.

DAHL R., HEIN K.A., SÉJOURNÉ S., OUÉDRAOGO C., GIOVENAZZO D. (2018). Geological, Structural, and Mineral Substances Synthesis Map of Burkina Faso at 1/1,000,000 Scale, Effigis Geo-Solutions Edition (In French).

DAHLIN T. (2004). A Numerical Comparison of 2D Resistivity Imaging with 10 Electrode Arrays, Geophysical Prospecting, Vol. 52, Issue 5, pp. 379–398.

DAKOURE D. (2003). Hydrogeological and Geochemical Study of the Southeastern Margin of the Taoudeni Sedimentary Basin (Burkina Faso-Mali): Modeling Attempt, Doctoral Thesis, Paris 6, France (In French).

DE CLERCQ T. (2021). Applied Geophysics for the Rehabilitation of Contaminated Sites, Doctoral Thesis, Normandie University, France (In French).

DE LASME O.Z., YOUAN TA M., BAKA D., ADOPO K.L., LASM T., OGA M.S. (2015). Quantitative evaluation and hydrogeochemical properties of groundwaters from precambrian rocks of San Pedro area (southwestern Côte d'Ivoire), Larhyss Journal, No 23, pp. 183-201.

DEWANDEL B. (2019). Basement Aquifers: Conceptual Models, Pumping Tests, and Regionalization of Hydrodynamic Properties, Doctoral Thesis, University of Montpellier, France (In French).

DOS SANTOS S. (2006). Access to Water and Socio-Sanitary Issues in Ouagadougou Burkina Faso, Space Populations Societies, University of Sciences and Technologies of Lille, France, Isue 2–3, pp. 271–285 (In French).

FAILLAT J.P., DROGUE C. (1993). Hydrochemical Differentiation of Superimposed Alterite and Fracture Aquifers in Granitic Basement, Hydrological Sciences Journal, Vol. 38, No 3, pp. 215–229.

FAYE M.D., BIAOU A.C., DOULKOM P.A., KOITA M., YACOUBA H. (2023). Contribution of Remote Sensing and Geophysical Prospecting (1D) to the Knowledge of Groundwater Resources in Burkina Faso, American Journal of Water Resources, Science and Education Publishing, Vol. 11, No 2, pp. 49–64.

FAYE M., BIAOU A., SORO D., LEYE B., KOITA M., YACOUBA H. (2020). Understanding Groundwater Pollution of the Sissili Catchment Area in Burkina Faso, Larhyss Journal, No 42, pp. 121–144.

FAYE M.D., KAFANDO M.B., SAWADOGO B., PANGA R., OUÉDRAOGO S., YACOUBA H. (2022). Groundwater Characteristics and Quality in the Cascades Region of Burkina Faso, Resources, Multidisciplinary Digital Publishing Institute, Vol. 11, No 7, p. 61.

FAYE M.D., LOYARA V.Y.B., BIAOU A.C., YONABA R., KOITA M., YACOUBA H. (2023). Modeling Groundwater Pollutant Transfer of Mineral Micropollutants in a Multi-Layered Aquifer in Burkina Faso (West African Sahel), Heliyon, Elsevier, Vol. 10, No 1.

GIOVENAZZO D., SÉJOURNÉ S., HEIN K A., JÉBRAK M., DAHL R., OUÉDRAOGO C., OUÉDRAOGO F., WENMENGA U. (2018). Explanatory Notice of the Geological, Structural, and Mineral Substances Synthesis Map of Burkina Faso at 1/1,000,000 Scale, Effigis Geo-Solutions Edition (In French).

HACINI M. (2006). Geochemistry of Salts and Brines of the Merouane Chott and Calculation of Precipitation Rates of Some Evaporite Minerals, Doctoral Thesis, University Badji Mokhtar of Annaba, Algeria (In French).

HIEN F., COMPAORE J.A., COULIBALY-SOME O. (1996). Soil Degradation Dynamics in the Nakambé Basin: A Diachronic Study in the Bissiga-Nakabé Classified Forest Area in Burkina Faso, Monitoring Soils in the Environment with Remote Sensing and GIS, Orstom Editions, Paris, pp. 523–30 (In French).

HOUNSINOU P., MAMA D., DOVONOU F., ALASANE A. (2015). Seasonal Evolution of the Microbiological Quality of Natural Waters in the Township of Abomey-Calavi (South Benin), British Journal of Earth Sciences Research, Vol. 3, No 1, pp. 30–41 (In French).

IHSAN T., DEROSYA V. (2024). Drinking water problems in rural areas: review of point-of-use methods to improve water quality and public health, Larhyss Journal, No 58, pp. 55-71.

IKEM A., OSIBANJO O., SRIDHAR M.K.C., SOBANDE A. (2002). Evaluation of groundwater quality characteristics near two waste sites in Ibadan and Lagos, Nigeria, Water, Air, and Soil Pollution, Springer, Vol. 140, No 1–4, pp. 307–333.

INSD (2020). Fifth General Census of Population and Housing of Burkina Faso: Preliminary Results of the 5th RGPH, 2019, National Institute of Statistics and Demography, 76 p (In French).

KOITA M., JOURDE H., RUELLAND D., KOFFI K., PISTRE S., SAVANE I. (2010). Mapping of regional accidents and identification of their role in the underground hydrodynamics in the basement zone. Case of the Dimbokro-Bongouanou region (Côte d'Ivoire), Hydrological Sciences Journal, Vol. 55, No 5, pp. 805–820 (In French).

KOUSSOUBE Y., SAVADOGO A.N., NAKOLENDOUSSE, S. AND BAZIE P. (2000). Efficiency of three geophysical lateral investigation methods in highlighting contacts between Lower Proterozoic geological formations in Burkina Faso: Evaluation of the efficiency of three geophysical methods for the determination of natural contacts between Lower Proterozoic geological formations of Burkina Faso, No 33, p. 13 (In French).

LACHACHE S., DERDOUR A., MAAZOUZI I., AMROUNE A., GUASTALDI E., MERZOUGUI T. (2023). Statistical Approach Of Groundwater Quality Assessment at Naama Region, South-West Algeria, Larhyss Journal, No 55, pp. 125–144.

LACHASSAGNE P., WYNS R. (2005). Basement aquifers, new concepts. Application to water resource prospecting and management, Géosciences, No 2, pp. 32–37.

LACHASSAGNE P., WYNS R., DEWANDEL B. (2011). The fracture permeability of hard rock aquifers is due neither to tectonics, nor to unloading, but to weathering processes, Terra Nova, Vol. 23, No 3, pp. 145–161.

LARISSA EBA A.E., KOUAME K.J., DEH S., BALLIET R., TOURÉ M., ANOH A.K., ROGER JOURDA J.P. (2016). Evaluation of the vulnerability to pollution of a surface water intended for potable water supply in a metropolis, Case of the Aghein Lagoon in Abidjan, (South of Côte d'Ivoire), European Scientific Journal, Vol. 12, No 36, p. 306 (In French).

LASM T. (2000). Hydrogeology of fractured basement reservoirs, statistical and geostatistical analysis of fracturing and hydraulic properties; application to the mountain region of Côte d'Ivoire (Archean domain), Doctoral thesis, Poitiers, France (In French).

LATER F., LABADI A.S. (2024). Origin of the alluvial aquifer's groundwater in wadi Biskra (Algeria), Larhyss Journal, No 57, pp. 145-158.

LGHOUL M., KCHIKACH A., HAKKOU R., ZOUHRI L., GUERIN R., BENDJOUDI H., TEIXIDO T., PENA J.A., ENRIQUE L., JAFFAL M. (2012). Geophysical and hydrogeological study of the abandoned mining site of Kettara (Marrakech, Morocco), contribution to the rehabilitation project, Hydrological Sciences Journal, Taylor & Francis, Vol. 57, No 2, pp. 370–381.

LOKE M.H. (2004). Tutorial, 2-D and 3-D electrical imaging surveys, Geotomo Software Compagny.

LOUKMAN B., NAKOLENDOUSSE S., NOUR A.M., NGUINAMBAYE, M.M. (2017). Hydrochemical characterization of the Yao aquifer and its surroundings: relationships between surface water (Lake Fitri) and groundwater, International

Journal of Biological and Chemical Sciences, Vol. 11, No 3, pp. 1336–1349 (In French).

MAHAMANE A.A., GUEL B. (2015). Physico-chemical characterizations of groundwater in Yamtenga locality (Burkina Faso), International Journal of Biological and Chemical Sciences, Vol. 9, No 1, pp. 517–533 (In French).

MAHAMAT S.A.M., MAOUDOMBAYE T., ABDELSALAM T., NDOUMTAMIA G., LOUKHMAN B. (2015). Evaluation of the physico-chemical quality of public water supply by the Chadian Water Company in N'Djamena, Chad, Journal of Applied Biosciences, Vol. 95, pp. 8973–8980 (In French).

MAJOLAGBE A.O., ADEYI A.A., OSIBANJO O., ADAMS A.O., OJURI O.O. (2017). Pollution vulnerability and health risk assessment of groundwater around an engineering landfill in Lagos, Nigeria, Chemistry International, Vol. 3, No 1, pp. 58–68.

METWALY M., ELAWADI E., MOUSTAFA S.S., AL ARIFI N., EL ALFY M., AL ZAHARANI EK. (2014). Groundwater contamination assessment in Al-Quwy'yia area of central Saudi Arabia using transient electromagnetic and 2D electrical resistivity tomography, Environmental earth sciences, Springer, Vol. 71, pp. 827–835.

MFONKA Z., NGOUPAYOU J.N., NDJIGUI P.D., ZAMMOURI M., KPOUMIE A., RASOLOMANANA E. (2015). Hydrochemistry and potability of water in the Nchi river basin in the Bamoun plateau (Western Cameroon), International Journal of Biological and Chemical Sciences, Vol. 9, No 4, pp. 2200–2218 (In French).

NAKOLENDOUSSE S., YAMÉOGO S., SAVADOGO A.N., KOUSSOUBE Y. (2009). Contribution of electrical and electromagnetic geophysical measurements to the study of the Samendéni dam site, highlighting faults and dolerite intrusions, Science and planetary changes/Sécheresse, Vol. 20, No 2, pp. 232–236 (In French).

NKHUWA D.C. (2003). Karstified marble terrain-an engineering geologic challenge of urban development in Lusaka, Zambia, Materials and Geoenvironment, Vol. 50, pp. 273–276.

NORONHA F., CATHELINEAU M., BOIRON M.-C., BANKS D.A., DÓRIA A., RIBEIRO M.A., NOGUEIRA P., GUEDES A. (2000). A three-stage fluid flow model for Variscan gold metallogenesis in northern Portugal, Journal of Geochemical Exploration, Elsevier, Vol. 71, No 2, pp. 209–224.

OLUSEYI T., ADETUNDE O., AMADI E. (2014). Impact assessment of dumpsites on the quality of nearby soil and underground water, a case study of an abandoned and a functional dumpsite in Lagos, Nigeria, International Journal Science Environment Technology, Vol. 3, No 3, pp. 1004–1015.

OSIBANJO O., MAJOLAGBE A.O. (2012). Physicochemical quality assessment of groundwater based on land use in Lagos city, southwest, Nigeria, Chemistry Journal, Vol. 2, No 2, pp. 79–86.

PARASNIS D.S. (1997). Principles of Applied Geophysics, Chapman and Hall, London, England, pp. 124–125.

PARASNIS D.S. (2012). Principles of applied geophysics, Springer Science & Business Media.

PATUREL J.E., BOUBACAR I., L'AOUR A., MAHE G. (2010). Analysis of rainfall grids and main features of changes that occurred in the 20th century in West and Central Africa, Hydrological Sciences Journal of Hydrological Sciences, Taylor & Francis, Vol. 55, No 8, pp. 1281–1288 (In French).

PENANT P. (2016). Characterization of nitrate sources in crystalline aquifers of central Benin, Doctoral thesis, University of Liège, Liège, Belgium (In French).

RABILOU S.M., MOUSBAHOU M.A.M., LAOUALI M.S., IBRAHIM N., HABOU I. (2018). Physico-chemical characterization of groundwater in the basement of the Zinder region (Niger) during the rainy and dry seasons, European Scientific Journal, Vol. 14, No 27, pp. 2395-2411 (In French).

REMINI B. (2010). The problem of water in northern Algeria, Larhyss Journal, No 8, pp. 27-46. (In French)

ROQUES C. (2013). Hydrogeology of fault zones in the crystalline basement: implications for water resources in the Armorican Massif, Doctoral Thesis, University of Rennes, France (In French).

SAKO A., YARO J.M., BAMBA O. (2018). Impacts of hydrogeochemical processes and anthropogenic activities on groundwater quality in the Upper Precambrian sedimentary aquifer of northwestern Burkina Faso, Applied Water Science, Springer, Vol. 8, No 3, p. 88.

SAVADOGO N. (1975). Hydrogeology of the Upper-Sissili watershed Upper Volta, Doctoral Dissertation, Scientific and Medical University of Grenoble, France (In French).

SAVADOGO N. (1984). Geology and hydrogeology of the crystalline basement of Upper Volta, Regional study of the Sissili watershed, Doctoral Dissertation, Scientific and Medical University of Grenoble, France (In French).

SAWADOGO B., FAYE M.D., KONATÉ Y., EKOUN A.L., AYELE G.T., KARAMBIRI H. (2023). Physico-Chemical and Microbial Characterisation of Water from the Abengourou Dam in Eastern Côte d'Ivoire, American Journal of Environmental Protection, Vol. 12, No 4, pp. 109–120.

SOGNON L. M., YALO N., LAWSON F. A., Alle, C. (2018). Geophysical characterization of salted bevel of the continental terminal aquifer at the southwestern edge of lake Nokoué in Benin. Larhyss Journal, No 34, pp. 69–95.

SONCY K., DJERI B., ANANI K., EKLOU-LAWSON M., ADJRAH Y., KAROU D.S., AMEYAPOH Y., DE SOUZA C. (2015). Evaluation of the bacteriological quality of well and borehole water in Lomé, Togo, Journal of Applied Biosciences, Vol. 91, pp. 8464–8469 (In French).

SORO D.D. (2017). Characterization and hydrogeological modeling of an aquifer in fractured bedrock, case of the experimental site of Sanon (central plateau region in Burkina Faso), Doctoral dissertation, Pierre and Marie Curie University-Paris VI, France, International Institute for Water and Environmental Engineering of Burkina Faso (In French).

SORO D. D., KOFFI K. V., et DIABATE A. (2020). Assessment of the geophysical location of water boreholes in a geological transition zone, Burkina Faso, Larhyss Journal, No 44, pp. 109–123.

SORO D.D., KOÏTA M., BIAOU C.A., OUTOUMBE E., VOUILLAMOZ J.-M., YACOUBA H., GUÉRIN R. (2017). Geophysical demonstration of the absence of correlation between lineaments and hydrogeologically useful fractures, case study of the Sanon hard rock aquifer (central northern Burkina Faso), Journal of African Earth Sciences, Elsevier, Vol. 129, pp. 842–852.

SORO N., OUATTARA L., DONGO K., KOUADIO E., AHOUSSI E., SORO G., OGA M., SAVANE I., BIEMI J. (2011). Municipal waste in the District of Abidjan in Côte d'Ivoire, potential sources of groundwater pollution, International Journal of Biological and Chemical Sciences, Vol. 4, No 6 (In French).

SOULEY MOUSSA R., MALAM ALMA M.M., LAOULI M.S., NATATOU I., HABOU I. (2019). Physico-chemical characterization of the waters of the Continental Intercalaire / Hamadien and the Continental Terminal aquifers in the Zinder region (Niger), International Journal of Biological and Chemical Sciences, Vol. 12, No 5, p. 2395 (In French).

VADDE K.K., WANG J., CAO L., YUAN T., MCCARTHY A.J., SEKAR R. (2018). Assessment of water quality and identification of pollution risk locations in Tiaoxi River (Taihu Watershed), China, Water, Multidisciplinary Digital Publishing Institute, Vol. 10, No 2, p. 183.

VALFREY-VISSER B., RAMA M. (2012). Country report - State of water and sanitation at the national level, Blue Book Burkina Faso, Second Edition (In French).

VOUILLAMOZ J.M., TOSSA A.Y.A., CHATENOUX B., KPEGLI K.A.R. (2015). Properties of Benin hard rock aquifers: multivariable and multiscale analysis of controlling parameters, Aquifers Bedrock Point on Concepts Operational Applications Roche-Sur-Yon (In French).

WAXMAN M.H., SMITS L. (1968). Electrical conductivities in oil-bearing shaly sands, Society of Petroleum Engineers Journal, Vol. 8, No 2, pp. 107–122.

WU M., LI W., DICK W.A., YE X., CHEN K., KOST D., CHEN L. (2017). Bioremediation of hydrocarbon degradation in a petroleum-contaminated soil and microbial population and activity determination, Chemosphere, Elsevier, Vol. 169, pp. 124–130.

YAMEOGO A., SOME Y.S.C., SIRIMA A.B., DA D.E.C. (2020). Land occupation and soil erosion in the upper Sissili watershed, Burkina Faso, Afrique Science, Vol. 17, No 5, pp. 43–56 (In French).

ZERHOUNI J., FILALI F.R., ABOULKACEM A. (2015). Quality and risk factors of groundwater pollution in the peri-urban area of Sebaa Ayoune (Meknes, Morocco), Larhyss Journal, No 22, pp. 91–107 (In French).

ZHANG H., GOODFELLOW I., METAXAS D., ODENA A. (2019). Self-attention generative adversarial networks, Proceedings of the 36th International Conference on Machine Learning, PMLR, Long Beach, California, USA, pp. 7354–7363.